ISSN 1990-3413, Astrophysical Bulletin, 2023, Vol. 78, No. 2, pp. 125–131. © Pleiades Publishing, Ltd., 2023.
Russian Text © Ivanoff, Petroff, Sidoroff ???, 2023, published in Astrofizicheskii Byulleten', 2023, Vol. 78, No. 2, pp. 00?–99?.

Searching for Brown Dwarfs in Large Photometric Surveys: WISE, 2MASS, AND DES

A. S. Avdeeva[1,2*], S. V. Karpov[3,4], and O. Yu. Malkov[1]

[1] *Institute of Astronomy, Russian Academy of Sciences, Moscow, 119017 Russia*

[2] *National Research University "Higher School of Economics", Moscow, 101000 Russia*

[3] *Special Astrophysical Observatory, Russian Academy of Sciences, Nizhnii Arkhyz, 369167 Russia*

[4] *Central European Institute of Cosmology and Fundamental Physics, Institute of Physics, Czech Academy of Sciences, Prague, 18221 Czech Republic*

Received December 15, 2022; revised January 25, 2023; accepted January 27, 2023

Abstract—Homogeneous and complete samples of brown dwarfs are needed for various kinds of studies: kinematic studies of the Galaxy, studies of binary stars with brown dwarfs, refinement of the low-mass end of the initial mass function, etc. According to various estimates, brown dwarfs can make up to 25% of the population of the Galaxy; however, the discovery of brown dwarfs with spectroscopic methods is extremely labor-intensive. In this paper, we present the cross-identification of the known nearest brown dwarfs from the 2021 list with the DES optical survey and the creation of photometric rules based on the detection of brown dwarfs in three surveys: WISE, 2MASS, and DES. Moreover, we present different photometric rules for each of the three families of brown dwarfs: bright, transit, and faint. No such division has been made yet.

DOI: 10.1134/S1990341323010017

Key words: *(stars): brown dwarfs—surveys—methods: data analysis*

1. INTRODUCTION

Brown dwarfs are substellar objects with masses between those that red M dwarfs and large planets have. However, their masses are still not enough to fuse and maintain the combustion of hydrogen in the core, so they cool down over time never reaching the Main Sequence.

Brown dwarfs were predicted theoretically (Hayashi and Nakano 1963; Kumar 1963) and then discovered 30 years later by (Rebolo et al. 1995). Since then, the search for new dwarfs (Burningham et al. 2013; Luhman 2013; Carnero Rosell et al. 2019) and the systematic study of the known brown dwarfs (Skrzypek et al. 2016; Kirkpatrick et al. 2021) have not stopped.

The discovery of new brown dwarfs helps to better determine their occurrence in the vicinity of the Sun and beyond. Knowledge of the spatial density and distribution of brown dwarfs provides key information about the distribution of mass in the Universe and the formation mechanism of brown dwarfs. Although thousands of brown dwarfs have been found over the past two decades, their number in the Sun's neighborhood is still in question (Robert et al. 2016).

This paper is devoted to the search for nearest brown dwarfs with significant proper motions. In our study, we rely on the "census" of brown dwarfs within 20 pc of the Sun compiled by Kirkpatrick et al. (2021), hereinafter, K2021.

This list contains the photometric data (2MASS (Skrutskie et al. 2006) and AllWISE (Cutri et al. 2021) magnitudes), the astrometric data (CatWISE (Marocco et al. 2021)), and the spectral classification for 496 brown dwarfs. We also cross-match the objects from K2021 with the DES DR1 (Abbott et al. 2018) survey. The transmission curves of the filters from the three surveys are presented in Fig. 1.

Based on the results of cross-matching, we have developed the rules which are descriptions of the boundaries of regions in the space of parameters (color indices) characteristic of the objects under study, and have carried out a trial search for objects that satisfy the developed rules in the 2MASS, AllWISE, and DES surveys. We have checked whether the data for the found objects are available in the Gaia DR3 catalog and concluded that the Gaia mission can be used for detection all the nearest brown dwarfs.

*E-mail: avdeeva@inasan.ru

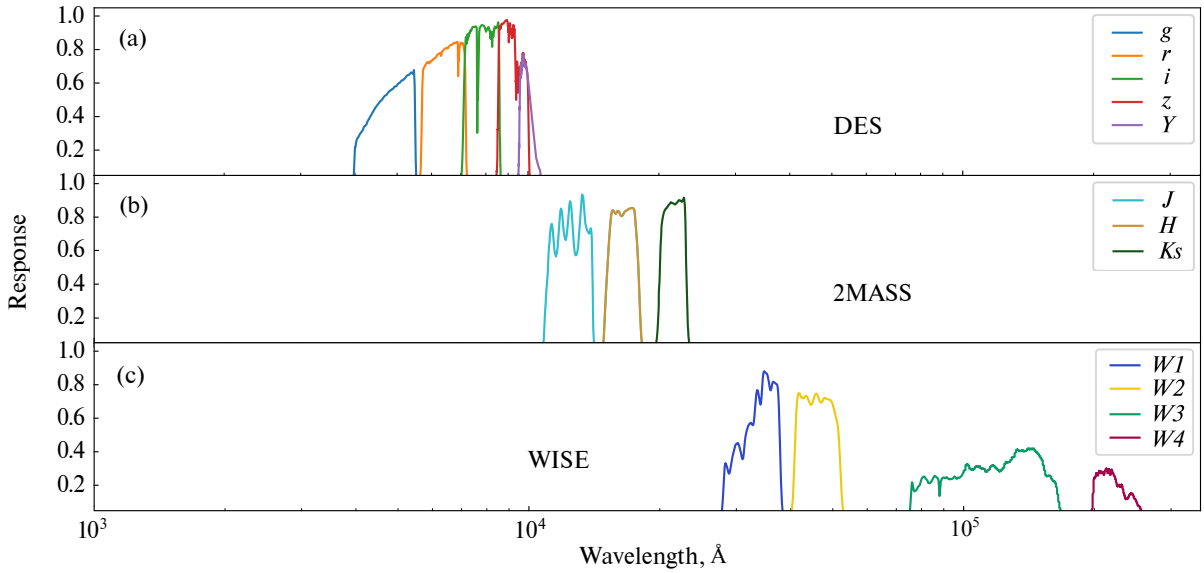

Fig. 1. Transmission curves of different surveys.

2. THREE FAMILIES OF BROWN DWARFS

According to Vos et al. (2019), brown dwarfs can be expected to manifest themselves in the parameter space (brightnesses and colors) in three different ways. It is all about the phenomenon called the L/T-transition: due to the complex atmospheric structure of cool dwarfs, their photometric properties change non-linearly with temperature (or spectral type).

Figure 2 shows the "temperature–spectral type" (panel (a)) and "color–spectral type" (panel (b)) diagrams for 496 brown dwarfs from K2021. The spectral type is encoded here as a number: $SpAd = 0$–9 for $L0$–$L9$, $SpAd = 10$–19 for $T0$–$T9$, and $SpAd = 20$–24 for $Y0$–$Y4$. There are two kinks in the "color–spectral type" diagram: between $L8$ and $L9$ and the next one between $T3$ and $T4$. As the effective temperature decreases, brown dwarfs first become redder (which corresponds to the shift of the Planck function maximum with decreasing temperature), and then, after the first kink, their color index $Ks{-}W1$ begins to shift towards a bluer color.

Finding the boundary of the next kink is not an easy task, since in this range the dispersion of color indices becomes quite significant. However, by combining this diagram with the "spectral type–temperature" diagram, we find that post-T3 brown dwarfs also exhibit behavior that differs from that of dwarfs of earlier spectral types. Thus, we divide our objects into three groups based on the value of $SpAd$: objects with $SpAd < 9$ we call bright, those with $9 \leq SpAd < 14$—transit, and with $SpAd \geq 14$—faint.

For each of these three families, we define photometric rules for cross-matching and searching in surveys independently of each other, since objects from different families often have different typical color indices and different interdependencies of color indices, which is confirmed in our paper. In addition, the search for objects by families allows us to primary make a rough spectral classification, since a certain range of spectral types corresponds to each family.

3. CROSS-MATCHING THE OBJECTS WITH THE DES CATALOG

Cross-matching the objects from multiple surveys is the process of establishing an unambiguous correspondence between observations of the same objects in different surveys. Often the most important thing in the process of cross-matching is the determination of the so-called cross-matching radius—the angular distance typical of the same objects in the given pair of surveys. However, the objects we study, being close to the Sun relative to most objects in the surveys[1], have large proper motions and can change their apparent position by tens of arcseconds during the time between observation epochs of different surveys used in this paper.

To cross-match the K2021 objects with the DES survey, we searched within a radius of 10″ using coordinates from the paper by Kirkpatrick et al. (2021) given for the epoch MJD 57170.5. In these circumstances, we were interested in all objects that fell within the region of the given radius, since we proceeded from the assumption that in the case of great proper motions, the nearest object from the survey

[1] The K2021 list includes the objects, whose distance does not exceed 20 pc.

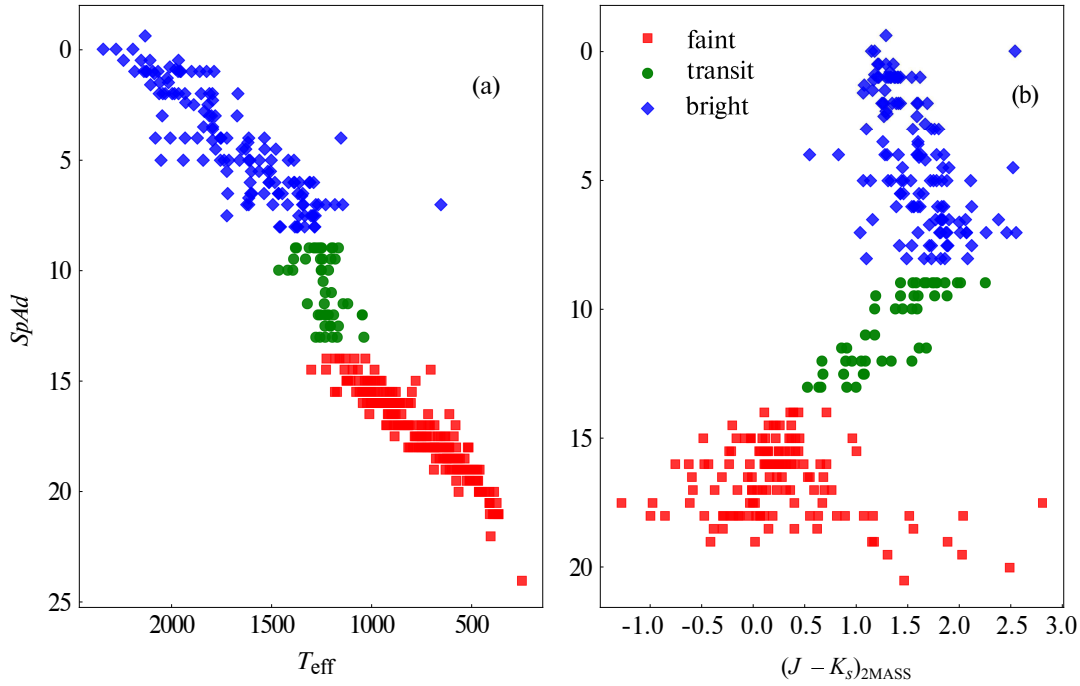

Fig. 2. Photometric, color, and spectroscopic characteristics of objects from three groups. Bright objects are marked in blue, transit objects in green, faint objects in red. See the description in the text.

of interest would not necessarily appear to be the correct matching. Thus, each object from the K2021 list, for which some matching from the DES catalog was found within a radius of 10″, can correspond to several entries in this catalog; from these entries we have to determine the correct matching. A special feature of the DES catalog is the impossibility to establish exactly when a particular object was observed or entry was done; so it is impossible to say with certainty whether the entries from the two catalogs: the K2021 and DES are correctly correlated in terms of coordinates, observation epochs, and proper motions. At the same time, knowing the epoch of the beginning and end of the DES mission observations (MJD 56519 and MJD 58492), it is possible to calculate, where on the celestial sphere the object should have been at the beginning and end of observations. To a first approximation, we compare the deviation (hereinafter Δ) of three resulting points (the "true" positions of the object at the start and end of the mission observations calculated from proper motions from the K2021, and the position of the object falling within a radius of 10″ of our search) from a straight line. The larger the deviation, the smaller the expectancy that this matching is correct.

Figure 3 shows a diagram of the $Y-J$ color index versus Δ (panel a) and the "color−color" $(z-Y, Y-J)$ diagram (panel b). We make the $\Delta < 4.2$ notch for all objects, among which we are looking for the correct matches, so that the dense group in the $(z-Y, Y-J)$ diagram unambiguously "passes" this filter. In this case, we believe that the increased density of objects in the region that falls into the selected area in the $(z-Y, Y-J)$ diagram indicates that these objects are more likely to be identified correctly.

We analyzed the positions of the objects left after the first filtering in five "color−color" diagrams: $(z-Y, Y-J)$, $(r-i, Y-J)$, $(Y-J, J-H)$, $(r-i, i-z)$, and $(i-z, z-Y)$ for outliers for each family separately.

Figure 4 shows an example of such outliers in the $(Y-J, J-H)$ diagram for objects of the bright and faint families. The circles indicate objects that we consider outliers and, therefore, incorrect identifications. Each object classified as an outlier in any diagram received a corresponding flag (each diagram has its own)[2]. The list, marked with flags, can later become the basis of a separate study, for example, in cases where the object is an outlier only in one diagram, and in the others it behaves in the same way as other brown dwarfs. The study of such objects is beyond the scope of this paper.

Thus, a match marked with at least one flag was considered unsuccessful at the moment and was not

[2]According to the diagram number, the maximum number of flags is 5.

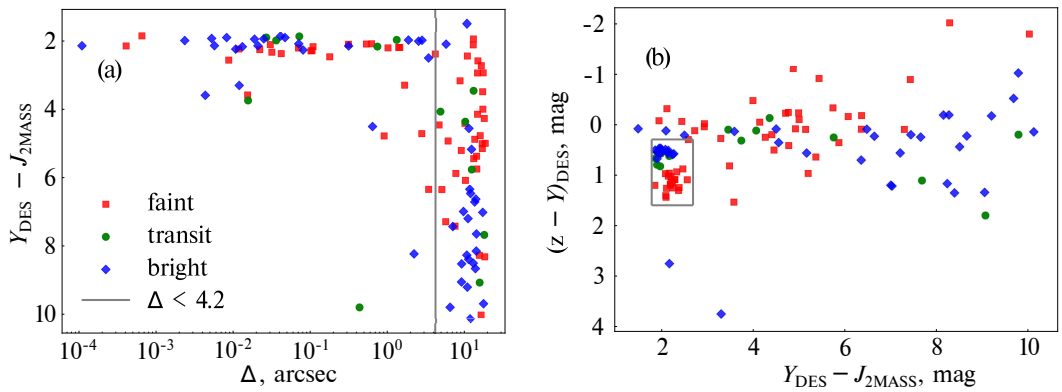

Fig. 3. Primary filtering of all objects within the search radius in the DES overview. The $\Delta < 4.2$ notch in the diagram on the left is made in such a way that all the objects from the marked area in the $(z - Y, Y - J)$ diagram on the right met this filter criterion.

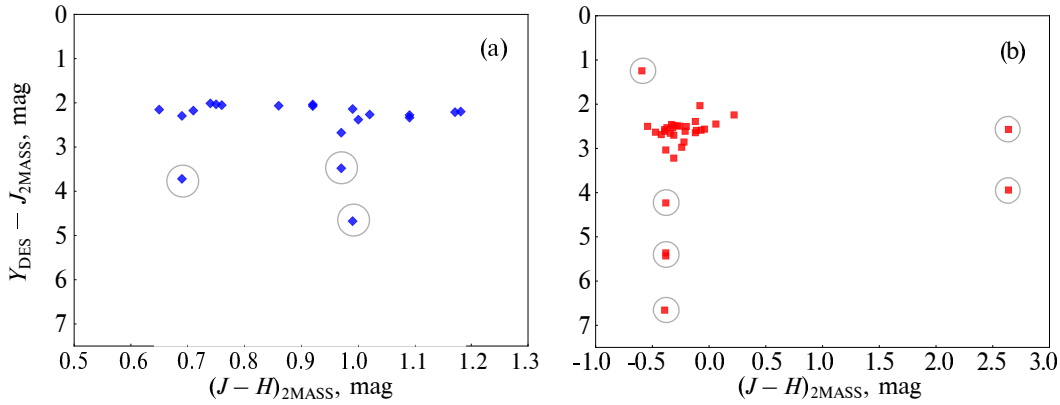

Fig. 4. Example of outliers in the diagrams for the case of the bright (a) and faint (b) families. The circled objects are are considered "suspicious" (most likely implausible) matches and are flagged.

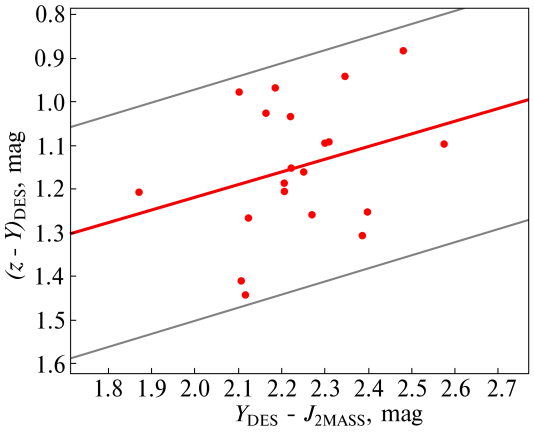

Fig. 5. Example of a photometric rule for finding faint-family brown dwarfs in the DES and 2MASS data. Straight lines show the area with "reliable" candidates (see the text).

taken into account in further work. In total, after analyzing five color diagrams, we still have 56 objects to study from the DES survey corresponding to the objects from K2021, of which 33 are faint, 18 are bright, and 5 are transit.

4. PHOTOMETRIC RULES

We excluded the outliers on all the diagrams and, in order to obtain photometric rules for searching for brown dwarfs in three surveys, described all regions in the "color – color" parameter space: $(J - H, H - K)$, $(H - K, K - W1)$, $(K - W1, W1 - W2)$, $(r - i, i - z)$, $(i - z, z - Y)$, $(z - Y, Y - J)$, $(r - i, Y - J)$, and $(Y - J, J - H)$. Each rule is a set of straight lines (vertical, horizontal, and oblique) limiting the area, in which the objects are located in the diagram.

Figure 5 shows an example of such a photometric rule. Since at the previous stage we removed all the objects considered unreliable, the lines are drawn in such a way that all the objects, for which the corresponding color indices can be calculated, fall inside the area. The inclination angle of the region boundaries is determined by the linear approximation

Table 1. Summary table of photometric rules for searching for brown dwarfs

Diagram	Bright	Transit	Weak
JHK	$-0.01 < (J-H)-(H-K) < 0.75$ $0.56 < (J-H) < 1.62$ $0.2 < (H-K) < 1.05$	$0.28 < (J-H)-0.9(H-K) < 1.03$ $0.4 < (J-H) < 1.6$ $0 < (H-K) < 0.84$	 $-0.9 < (J-H) < 1$ $-1.4 < (H-K) < 2.7$
$HKW1$	$0.05 < (H-K)-0.42(K-W1) < 0.6$ $0.56 < (J-H) < 1.62$ $0.2 < (H-K) < 1.05$	$-0.42 < (H-K)-0.78(K-W1) < 0.16$ $0.4 < (J-H) < 1.6$ $0 < (H-K) < 0.84$	$0.55 < (H-K)+0.83(K-W1) < 2.15$ $-0.9 < (J-H) < 1$ $-1.4 < (H-K) < 2.7$
$KW1W2$	$-0.3 < (K-W1)-1.62(W1-W2) < 0.45$ $0.26 < (K-W1) < 1.24$ $0.17 < (W1-W2) < 0.67$	$0.7 < (K-W1)+0.44(W1-W2) < 1.4$ $0.35 < (K-W1) < 1.15$ $0.33 < (W1-W2) < 1.32$	$-0.75 < (K-W1)+0.29(W1-W2) < 3$ $-1.7 < (K-W1) < 2$ $0.7 < (W1-W2) < 4.4$
$W1W2W3$	 $0.18 < (W1-W2) < 0.67$ $-0.44 < (W2-W3) < 1.29$	 $0.3 < (W1-W2) < 1.32$ $0.54 < (W2-W3) < 1.68$	$0.3 < (W1-W2)-0.46(W2-W3) < 3.9$ $1.1 < (W1-W2) < 4.7$ $0.7 < (W2-W3) < 3.5$
riz	$0.01 < (r-i)-0.69(i-z) < 1.4$ $1 < (r-i) < 2.65$ $1.2 < (i-z) < 2.25$	 $2.05 < (r-i) < 4.45$ $2.15 < (i-z) < 3.05$	$-2.8 < (r-i)-0.6(i-z) < 5.2$ $-0.2 < (r-i) < 7.4$ $0.3 < (i-z) < 4.45$
izY	$1.2 < (i-z) < 2.25$ $0.45 < (z-Y) < 0.7$	$2.15 < (i-z) < 3.05$ $0.57 < (z-Y) < 0.84$	$0.3 < (i-z) < 4.45$ $0.7 < (z-Y) < 1.55$
zYJ	 $0.45 < (z-Y) < 0.7$ $1.86 < (Y-J) < 2.3$	 $0.57 < (z-Y) < 0.84$ $1.85 < (Y-J) < 2.2$	$1.57 < (z-Y)+0.29(Y-J) < 2.07$ $0.7 < (z-Y) < 1.55$ $1.8 < (Y-J) < 2.6$
$riYJ$	$1 < (r-i) < 2.65$ $1.86 < (Y-J) < 2.3$	$2.05 < (r-i) < 4.45$ $1.85 < (Y-J) < 2.2$	$-0.2 < (r-i) < 7.4$ $1.8 < (Y-J) < 2.6$
YJH	$1.4 < (Y-J)-0.46(J-H) < 1.8$ $1.86 < (Y-J) < 2.3$ $0.56 < (J-H) < 1.62$	 $1.85 < (Y-J) < 2.2$ $0.4 < (J-H) < 1.6$	$2 < (Y-J)+0.31(J-H) < 2.55$ $1.8 < (Y-J) < 2.6$ $-0.9 < (J-H) < 1$

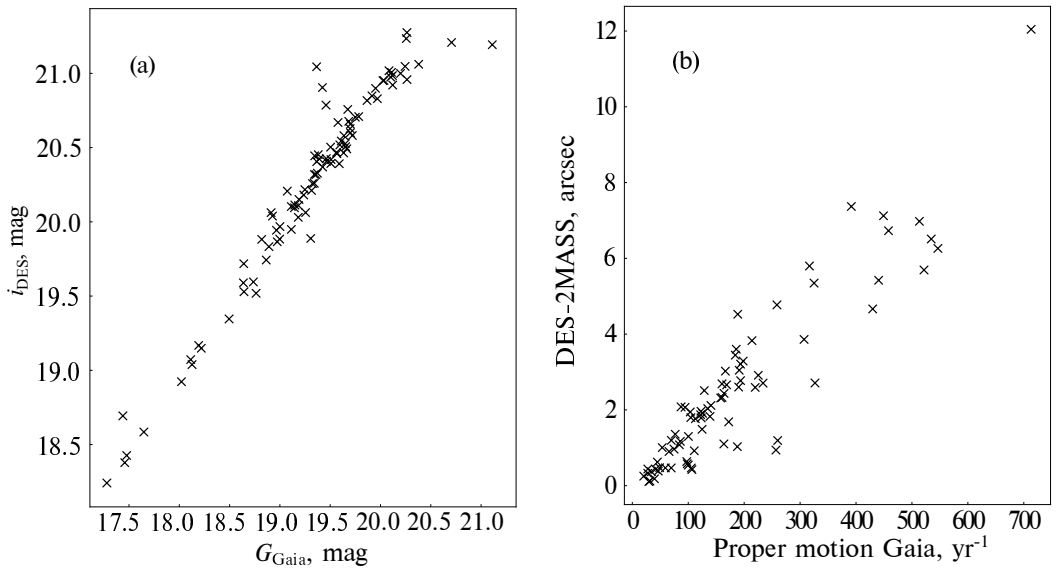

Fig. 6. Comparison of the data on potential brown dwarfs and identification with Gaia: photometry (a) and proper motion (b).

of the color indices. If the inclination angle is $k < 0.1$, then we consider that it is inexpedient to carry out linear approximation, and we limit the region to only horizontal and vertical lines. Table 1 shows the entire list of the given rules.

5. SEARCH FOR BROWN DWARFS AND COMPARISON WITH GAIA DR3

We carried out a trial search for brown dwarfs in the AllWISE, 2MASS, and DES DR1 surveys. Comparing the entries in the surveys within a radius of 50″, we chose only those that fit the rules we have developed.

The primary search gave us 174 entries that matched our criteria. We then checked the coordinates of supposedly the same object in different surveys to see if they correspond to the object's proper motion. The distance of positions from the big circle drawn through the positions in DES and 2MASS was determined using the AllWISE coordinates; and all the objects, where this distance was greater than 1″, were discarded. There were 137 of 174 objects left. We then compared the distances of the DES point from those of AllWISE and 2MASS. The distance to the position in AllWISE should be between 0.2 and 0.35 of the distance from 2MASS (because we do not know the individual observation epochs in DES). We checked whether the AllWISE position falls within this interval, taking 2MASS and AllWISE 1″ for positional accuracy, and considering DES to be conditionally absolutely accurate. This omitted two more objects. As a result, we have 135 candidates which do not positionally contradict the hypothesis of their proper motions.

For the primary analysis of the obtained objects, we took the cross-matching according to the coordinates with a radius of 1.″5, given in NOIRLab's Astro Data Lab[3]. Such a matching is available for 96 objects out of 135. Since a simple cross-matching by coordinates may not give a good result, we compared the brightnesses of objects in DES and their matchings in Gaia (Fig. 6a). Most objects show good agreement in the brightnesses $i_{\rm DES}$ and $G_{\rm Gaia}$. It can be seen that the discrepancy is greater, the smaller the brightness of the object in both surveys. Figure 6b shows a matching of the distances between the positions of objects in DES and 2MASS and proper motions from Gaia. The compared values basically coincide qualitatively, and, taking into account the average difference in the epoch of the surveys, also quantitatively.

We also compared the objects, for which there were and were not found matches in Gaia, in terms of proper motion and brightness (Fig. 7). The proper motions in this case are calculated conditionally based on the position distances in the DES and 2MASS surveys and the average epoch difference of 15 years. As can be seen from the distribution of proper motions, large proper motions are not the reason why no data have been found for 39 objects in the Gaia archive. In contrast to proper motions, the brightnesses of objects, for which a matching has been obtained in Gaia and no such matching has been found, differ significantly. Despite some exceptions, the "found" objects are on average brighter than other objects. On this basis, we conclude that the Gaia's

[3] https://datalab.noirlab.edu/gaia.php

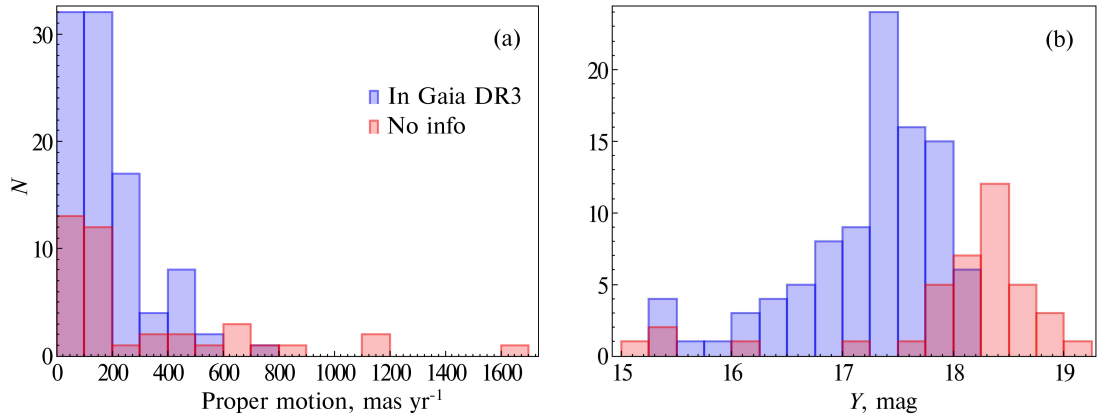

Fig. 7. Distributions for objects present and absent in the Gaia archive: according to the proper motions calculated from the distance between the positions in the DES and 2MASS surveys, and brightnesses according to the DES data, panels (a) and (b), respectively.

depth may not be sufficient to identify at least a third of brown dwarfs.

6. CONCLUSION

This paper presents the development of the photometric rules for searching for brown dwarfs in the WISE, 2MASS, and DES surveys and the primary search based on these rules. In order to develop photometric rules, the brown dwarf census in the nearest 20 pc (K2021) was cross-matched with the DES survey. The photometric rules have been developed for three families of brown dwarfs: faint, transit, and bright, according to their photometric features.

According to the developed rules, a trial search for brown dwarfs was carried out in the three surveys taking into account the fulfillment of all the rules. The matching was found from the Gaia DR3 catalog for 96 out of 135 objects that meet our criteria within a radius of 1″.5. The proper motions of our objects, calculated from the difference of positions in the 2MASS and DES surveys, agree qualitatively and quantitatively with the Gaia measurements. Another 39 objects for which no matching was found in Gaia appear to be too faint for this survey. Thus, the data from the Gaia mission only will not be sufficient to detect all the nearby brown dwarfs.

ACKNOWLEDGMENTS

The authors are grateful to the reviewer for careful reading of the paper and comments made.

FUNDING

The work was supported by the Ministry of Science and Higher Education of the Russian Federation within the framework of the grant No. 075-15-2022-1228 (13.2251.21.0177).

CONFLICT OF INTEREST

The authors declare no conflict of interest regarding the publication of this paper.

REFERENCES

1. T. M. C. Abbott, F. B. Abdalla, S. Allam, et al., Astrophys. J. Suppl. **239** (2), article id. 18 (2018).
2. B. Burningham, C. V. Cardoso, L. Smith, et al., Monthly Notices Royal Astron. Soc. **433** (1), 457 (2013).
3. A. Carnero Rosell, B. Santiago, M. dal Ponte, et al., Monthly Notices Royal Astron. Soc. **489** (4), 5301 (2019).
4. R. M. Cutri, E. L. Wright, T. Conrow, et al., VizieR Online Data Catalog II/328 (2021).
5. C. Hayashi and T. Nakano, Progress of Theoretical Physics **30** (4), 460 (1963).
6. J. D. Kirkpatrick, C. R. Gelino, J. K. Faherty, et al., Astrophys. J. Suppl. **253** (1), id. 7 (2021).
7. S. S. Kumar, Astrophys. J. **137**, 1121 (1963).
8. K. L. Luhman, Astrophys. J. **767** (1), article id. L1 (2013).
9. F. Marocco, P. R. M. Eisenhardt, J. W. Fowler, et al., Astrophys. J. Suppl. **253** (1), id. 8 (2021).
10. R. Rebolo, M. R. Zapatero Osorio, and E. L. Martín, Nature **377** (6545), 129 (1995).
11. J. Robert, J. Gagné, É. Artigau, et al., Astrophys. J. **830** (2), article id. 144 (2016).
12. M. F. Skrutskie, R. M. Cutri, R. Stiening, et al., Astron. J. **131** (2), 1163 (2006).
13. N. Skrzypek, S. J. Warren, and J. K. Faherty, Astron. and Astrophys. **589**, id. A49 (2016).
14. J. M. Vos, K. Allers, D. Apai, et al., Bull. Amer. Astron. Soc. **51** (3), id. 253 (2019).

Translated by N. Oborina